Spin analyzing power for polarized top decays with jets

Yoshio Kitadono[1,*] and Hsiang-nan Li[1,2,3,†]

[1]*Institute of Physics, Academia Sinica, 128, Section 2, Academia Road, Nankang, Taipei 11529, Taiwan, Republic of China*
[2]*Department of Physics, National Cheng-Kung University, Tainan, Taiwan 701, Republic of China*
[3]*Department of Physics, National Tsing-Hua University, Hsin-Chu, Taiwan 300, Republic of China*

We perform perturbative QCD factorization of infrared radiations associated with an energetic b quark from a polarized top quark decay, taking the semileptonic channel as an example. The resultant formula is expressed as a convolution of an infrared-finite heavy-quark kernel with a b-quark jet function. Evaluating the heavy-quark kernel up to leading order in the coupling constant and adopting the jet function from QCD resummation, we predict the dependence of the spin analyzing power for a polarized top quark on the invariant mass of the b-quark jet. It is observed that the spin analyzing power could be enhanced by a factor 2 compared to the inclusive case with the jet mass being integrated over. It is worthwhile to test experimentally the enhancement of the spin analyzing power due to the inclusion of jet dynamics.

I. INTRODUCTION

A study of the top quark physics contributes to the understanding of the origin of the electroweak symmetry breaking in the standard model and its extensions. Progress in this field from the Large Hadron Collider (LHC), a top quark factory, has been reviewed in Refs. [1,2]. Higher-order calculations of top production and decay processes were summarized in Ref. [3] (see also references therein). Especially, observables related to the spin of a top quark may reveal various new physics effects, which can be explored at LHC (for recent references, refer to Ref. [4]). Since a top quark decays almost 100% into a b quark and a W boson before hadronization, one can extract the information on the spin of a ''bare top quark'' from the angular distribution of its decay products. For this purpose, the spin analyzing power κ_i for a final state i in a polarized top quark decay has been defined via

$$\frac{1}{\Gamma}\frac{d\Gamma}{d\cos\theta_i} = \frac{1}{2}(1 + \kappa_i|\vec{P}|\cos\theta_i), \qquad (1)$$

where Γ is the partial decay width, $\vec{P}$ is the polarization vector of a polarized ensemble of top quarks at rest with $0 \le |\vec{P}| \le 1$, and θ_i is the angle of the particle momentum measured from the top quark spin. That is, κ_i relates the top quark spin to the angular distribution of the decay product i.

QCD corrections to the polarized $t \to bW^+$ decay were investigated in Ref. [5], and those to the spin analyzing power were done for semileptonic decays in Refs. [6,7], and for hadronic decays in Ref. [8]. The results have been summarized in Table 3 of Ref. [2]: charged leptons and down-type quarks exhibit the largest power ($\kappa \simeq 1$), a bottom quark has a second-largest power ($\kappa \simeq -0.4$),

neutrinos and up-type quarks have a value of $\kappa \simeq -0.3$, and the less energetic non-b jet shows $\kappa \simeq 0.5$ [9]. It was observed that next-to-leading-order (NLO) corrections to the spin analyzing power are not important, and the b quark mass could be safely ignored in the above analysis of the polarized top quark decay [8]. Although the light-particle jets from the u and d quarks have been considered, the spin analyzing power associated with the b-quark jet is not known yet. In particular, a jet mass can be measured, so it is interesting to examine how the spin analyzing power for a polarized top quark depends on the b-quark jet mass. This is the motivation of the present work.

A fundamental framework for studying high-energy processes is the perturbative QCD (pQCD) factorization theorem [10–12], in which cross sections and decay widths are factorized into convolutions of several subprocesses. Take top quark decays as an example. The subprocesses include jet functions which contain infrared radiations associated with energetic hadronic final states, soft functions which collect infrared gluons exchanged among the top quark and hadronic final states, and heavy-quark kernels from the difference between the QCD diagrams for the top quark decays and the effective diagrams for the jet and soft functions. In this paper we shall demonstrate the factorization of the b-quark jet from the semileptonic top quark decay, that requires the eikonal approximation for particle propagators in infrared regions and on the Ward identity for organizing all diagrams with attachments of infrared gluons [13]. The soft functions will be neglected here due to the cancellation between virtual and real corrections, and to the fact that they have minor effects on jet mass distributions. The pQCD factorization formula for the semileptonic decay of a polarized top quark is then expressed as a convolution of the infrared-finite heavy-quark kernel with the b-quark jet function.

It has been known that the overlap of collinear and soft dynamics produces large double logarithms in a jet

---

*kitadono@phys.sinica.edu.tw
†hnli@phys.sinica.edu.tw

function, which should be summed up to all orders. References on the resummation of various double logarithms can be found in Refs. [14–18]. Recently, the QCD resummation technique for light-particle jets has been developed [19,20], by means of which jet substructures, such as jet mass distributions and energy profiles, can be calculated. Substituting the quark jet function derived in Ref. [20] into the pQCD factorization formula for the polarized top quark decay, we show that the spin analyzing power increases with the jet mass quickly, and is possibly enhanced by a factor 2 in a wide range of the jet mass. This result is attributed to the observation that the shape of the jet function puts more weight on the contribution from the kinematic region with higher b-quark jet momentum, where the spin analyzing power is larger. It is worthwhile to test experimentally the enhancement of the spin analyzing power due to the inclusion of jet dynamics.

The pQCD factorization of the b-quark jet function from the semileptonic decay of a polarized top quark is performed up to NLO by employing the eikonal approximation in Sec. II. The procedures that rely on the application of the Ward identity for the all-order factorization are outlined. The doubly differential width for the angular distribution of the b-quark jet with a specified invariant mass is presented in Sec. III. We propose a parametrization for the quark jet function derived in Ref. [20] in order to simplify numerical analysis. The choices of physical parameters and our predictions are summarized. Section IV is devoted to a conclusion.

II. FORMALISM

We consider the semileptonic top quark decay,

$$t(k_t, s_t) \rightarrow b(k_b) + \ell^+(k_\ell) + \nu_\ell(k_\nu), \quad (2)$$

where k_t, k_b, k_ℓ, and k_ν are the momenta of the top quark, the b quark, the charged lepton, and the neutrino, respectively, as indicated in Fig. 1 for the leading-order (LO) amplitude. In this section we shall identify the leading infrared contributions, and perform their factorization into the b-quark jet function.
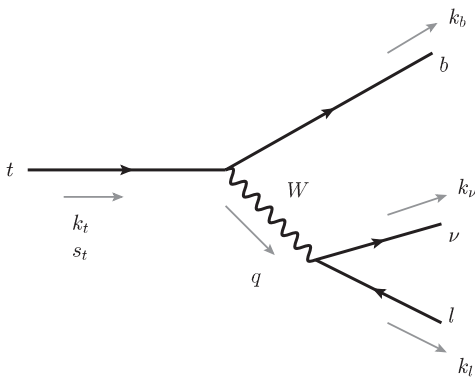
A. Factorization at LO

The averaged decay amplitude squared $|\overline{\mathcal{M}}_0|^2$ at LO in both the electroweak coupling and the strong coupling, depicted in Fig. 2, is written as

$$|\overline{\mathcal{M}}_0|^2 = \frac{1}{4} \frac{g^4 |V_{tb}|^2}{(q^2 - m_W^2)^2 + m_W^2 \Gamma_W^2} L_{\mu\rho} T^{\mu\rho}, \quad (3)$$

with the leptonic and hadronic tensors

$$
\begin{aligned}
L_{\mu\rho} &= d_{\mu\nu} d_{\rho\sigma} \mathrm{tr}[\gamma^\nu P_L \slashed{k}_l \gamma^\sigma P_L \slashed{k}_\nu], \\
T^{\mu\rho} &= \mathrm{tr}[\gamma^\mu P_L \hat{w}_t (\slashed{k}_t + m_t) \gamma^\rho P_L (\slashed{k}_b + m_b)].
\end{aligned}
\quad (4)
$$

In the above expression, g is the gauge coupling of the weak interaction, V_{tb} is the Cabibbo-Kobayashi-Maskawa matrix element, $q = k_t - k_b = k_\nu + k_\ell$, m_W and Γ_W are the momentum, the mass, and the decay width of the W boson, respectively, $d_{\mu\nu} = g_{\mu\nu} - q_\mu q_\nu / m_W^2$ arises from the summation over the polarizations of the W boson, $P_L = (1 - \gamma^5)/2$ is the projection matrix, $\hat{w}_t = (1 + \gamma_5 \slashed{s}_t)/2$ is the spin projector for the top quark, m_t and m_b are the masses of the top quark and the b quark, respectively, and the lepton masses have been dropped.

The three-body phase-space integral for the top quark decay is given by

$$
\begin{aligned}
\int d\mathrm{PS}^{(3)} &= \int \frac{1}{2E_b} \frac{d^3\vec{k}_b}{(2\pi)^3} \frac{1}{2E_\ell} \frac{d^3\vec{k}_\ell}{(2\pi)^3} \frac{1}{2E_\nu} \frac{d^3\vec{k}_\nu}{(2\pi)^3} (2\pi)^4 \\
&\quad \times \delta^4(k_t - k_b - k_\ell - k_\nu), \\
&= \pi \int \frac{dE_b d\cos\theta_b}{2(2\pi)^2} \frac{dE_\ell d\chi}{2(2\pi)^3},
\end{aligned}
\quad (5)
$$

with E_i being the energy of the particle i, $i = b, \ell, \nu$. The angle θ_b is the polar angle of the b quark with respect to the top quark spin as indicated in Fig. 3, the azimuthal angle ϕ_b has been integrated out, and χ denotes the angle between the $\vec{s}_t$-$\vec{k}_b$ plane and the $\vec{k}_b$-$\vec{k}_\ell$ plane.

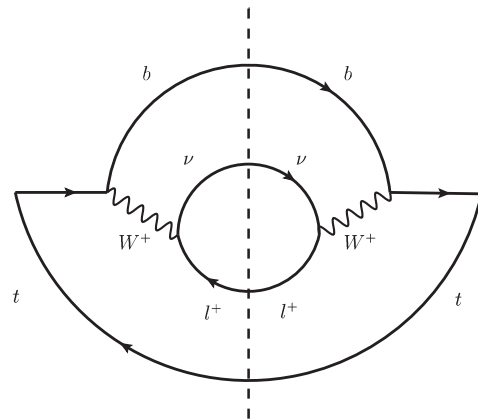FIG. 1.   LO amplitude for the semileptonic top quark decay.

FIG. 2.   LO decay width for the semileptonic top quark decay, where the vertical dashed line represents the final-state cut.
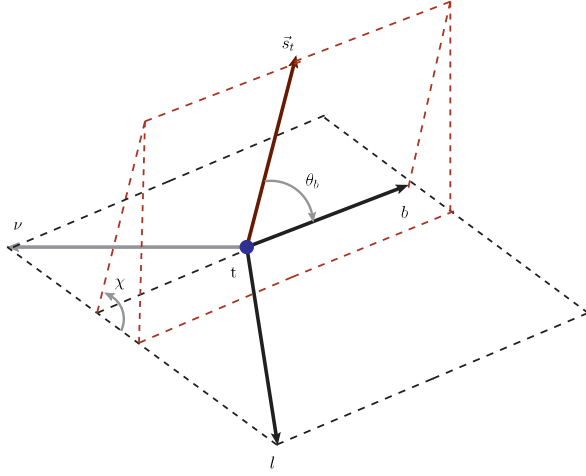
FIG. 3 (color online).   Angles of final-state particles defined in the rest frame of the top quark.

FIG. 4.   Factorization of the b-quark jet from the LO diagram for the decay width.

We insert the identity,

$$\int dm_J^2 dE_J d^2\hat{n}_J \delta(m_J^2 - m_b^2)\delta(E_J - E_b)\delta^{(2)}(\hat{n}_J - \hat{n}_b) = 1, \tag{6}$$

into the differential decay width, where m_J (E_J) is the jet invariant mass (energy), and the jet (b-quark) direction is defined by $\hat{n}_J = \vec{k}_J/|\vec{k}_J|$ ($\hat{n}_b = \vec{k}_b/|\vec{k}_b|$). The three δ functions in Eq. (6), together with the b-quark phase space, are absorbed into the LO b-quark jet function $J^{(0)}(m_J^2, E_J, R)$, which will be specified later. We further factorize the fermion flow in Eq. (4) by applying the Fierz transformation,

$$I_{ij}I_{lk} = \frac{1}{4}I_{ik}I_{lj} + \frac{1}{4}(\gamma_5)_{ik}(\gamma_5)_{lj} + \frac{1}{4}(\gamma_\alpha)_{ik}(\gamma^\alpha)_{lj}$$
$$+ \frac{1}{4}(\gamma_5\gamma_\alpha)_{ik}(\gamma^\alpha\gamma_5)_{lj} + \frac{1}{8}(\sigma_{\alpha\beta})_{ik}(\sigma^{\alpha\beta})_{lj}, \tag{7}$$

with I being the identity matrix and $\sigma_{\alpha\beta} \equiv i[\gamma_\alpha, \gamma_\beta]/2$. The vectors

$$\xi_J = \frac{1}{\sqrt{2}}(1, -\hat{n}_J), \qquad \bar{\xi}_J = \frac{1}{\sqrt{2}}(1, \hat{n}_J) \tag{8}$$

are introduced, which lie on the light cone and satisfy $\xi_J\bar{\xi}_J = 1$. The third term in Eq. (7), especially the component $(\xi_J)_{ik}(\bar{\xi}_J)_{lj}/4$, gives the leading-power contribution. The matrix $\xi_J/2$ goes into the trace for the b-quark jet function, and the matrix $\bar{\xi}_J/2$ goes into the trace for the heavy-quark kernel. We also employ the identity,

$$I_{ij}I_{lk} = \frac{1}{N_c}I_{ik}I_{lj} + 2\sum_c(T^c)_{ik}(T^c)_{lj}, \tag{9}$$

to factorize the color flow, where I_{ik}/N_c goes into the b-quark jet function, and I_{lj} goes into the heavy-quark kernel. The fermion and color traces between the b-quark jet function and the heavy-quark kernel are then separated.
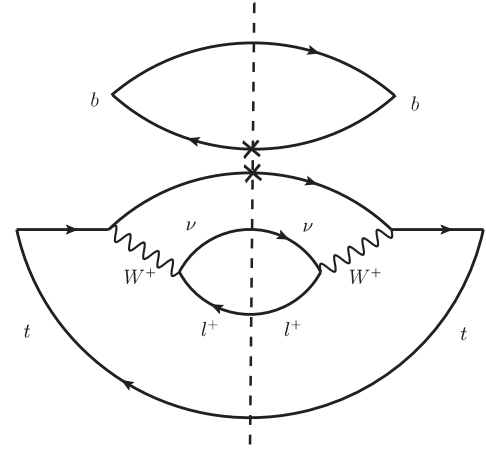
Figure 2 becomes Fig. 4, where the cross vertex stands for the insertion of the gamma matrices from the Fierz transformation. The differential decay width is factorized at LO into

$$d\Gamma^{(0)}(t \to b\ell\nu)$$
$$= \frac{\sqrt{2}\pi}{(2\pi)^5}\left(\frac{m_t}{2}\right)^3 d\cos\theta_J dm_J^2 \frac{x_J dx_J}{\sqrt{1 - 4z_J/x_J^2}} dx_\ell d\chi \tag{10}$$

$$\times H^{(0)}(k_t, k_\ell, k_J)J^{(0)}(m_J^2, E_J, R), \tag{11}$$

with the LO heavy-quark kernel

$$H^{(0)} = \frac{1}{4}\frac{g^4|V_{tb}|^2}{(q^2 - m_W^2)^2 + m_W^2\Gamma_W^2}d_{\mu\nu}d_{\rho\sigma}\text{tr}[\gamma^\nu P_L \slashed{k}_\ell \gamma^\sigma P_L \slashed{k}_\nu]$$
$$\times \text{tr}\left[\gamma^\mu P_L \hat{w}_t(\slashed{k}_t + m_t)\gamma^\rho P_L \frac{1}{2}\slashed{\xi}_J\right],$$
$$= \frac{g^4|V_{tb}|^2}{2\sqrt{2}}\frac{1}{m_t}\frac{1}{x_J}f(x_\ell, x_J; z_J)(1 + |\vec{P}|\cos\theta_\ell), \tag{12}$$

and the function

$$f(x_\ell, x_J; z_J) = \frac{x_\ell(1 - x_\ell - z_J)}{(1 + z_J - x_J - \xi)^2 + \xi^2\eta^2}. \tag{13}$$

In the above expression the dimensionless variables are defined as

$$x_J = \frac{2E_J}{m_t}, \quad x_\ell = \frac{2E_\ell}{m_t}, \quad z_J = \frac{m_J^2}{m_t^2}, \quad \xi = \frac{m_W^2}{m_t^2}, \quad \eta = \frac{\Gamma_W}{m_W}, \tag{14}$$

and the LO jet function $J^{(0)}$ is equal to the δ function, $J^{(0)} = \delta(m_J^2 - m_b^2)$. It is easy to see that Eq. (12) is consistent with the fixed-order calculations in Refs. [6,21].

B. Factorization at NLO

We then consider radiative corrections to the above LO decay width, which involves two dramatically different scales, the top quark mass m_t and the b-quark mass m_b. Since the b-quark mass will be neglected eventually, m_b and the QCD scale will not be differentiated here. There are two leading infrared regions for a loop momentum l, in which the radiative gluon is off shell by $l^2 \sim O(m_b^2)$. The collinear region corresponds to l collimated to k_b, namely, $k_b l \sim O(m_b^2)$. Another is the soft region defined in the heavy-quark effective theory, where the gluon momentum scales like $l^\mu \sim O(m_b)$ with $k_b l \sim O(m_t m_b)$. Collinear gluons can be factorized from the top quark decay amplitude into the b-quark jet function $J(m_J^2, E_J, R)$ with the jet cone of radius R. Soft gluons, except those emitted into the jet cone, will be ignored as explained in the Introduction. Hence, we focus on the factorization of the b-quark jet function below.

For the factorization at NLO, we first consider a virtual gluon emitted by the top quark and attaching to the b quark. In the collinear region, where the loop momentum l carries a large component of $O(m_t)$ along the b quark momentum, we have the hierarchy $k_t l \sim O(m_t^2) \gg l^2 \sim O(m_b^2) \sim O(m_J^2)$. It implies that the collinear gluon can be factorized into the NLO virtual b-quark jet function $J^{(1)v}(m_J^2, E_J, R)$ by means of the eikonal approximation, under which the virtual top quark propagator is simplified into $\xi_J/\xi_J l$. It means that the collinear gluon has been detached from the top quark line, and collected by a Wilson line in the direction of ξ_J. The separation of the fermion flow and the color flow between the jet function and the heavy-quark kernel also follows Eqs. (7) and (9), respectively. Associating the three δ functions in Eq. (6) with the NLO jet function, the differential decay width with the above virtual correction is written, at leading power of m_J/m_t, as the convolution

$$d\Gamma^{(1)v}(t \to b\ell\nu)$$
$$= \frac{\sqrt{2}\pi}{(2\pi)^5}\left(\frac{m_t}{2}\right)^3 d\cos\theta_J dm_J^2 \frac{x_J dx_J}{\sqrt{1 - 4z_J/x_J^2}} dx_\ell d\chi$$
$$\times [H^{(0)}(k_t, k_\ell, k_J)J^{(1)v}(m_J^2, E_J, R)$$
$$+ H^{(1)v}(k_t, k_\ell, k_J)J^{(0)}(m_J^2, E_J, R)]. \qquad (15)$$

The infrared-finite NLO virtual heavy-quark kernel $H^{(1)v}$ is defined as the difference between the left-hand side and the first term on the right-hand side via the above expression.

We then consider the QCD correction, where a real gluon is emitted by the top quark and attaches to the b quark. The hierarchy $k_t l \sim O(m_t^2) \gg l^2 = 0$ $[k_t l \sim O(m_t m_b) \gg l^2 = 0]$ for a real gluon automatically holds in the collinear (soft) region, implying the factorization of the infrared gluon into the b-quark jet function

through the eikonalization of the top quark propagator. In this case we insert the identity,

$$\int dm_J^2 dk_J^0 d^2\hat{n}_J \delta(m_J^2 - (k_b + l)^2)$$
$$\times \delta(k_J^0 - k_b^0 - l^0)\delta^{(2)}(\hat{n}_J - \hat{n}_{b+g}) = 1, \qquad (16)$$

to define the NLO real b-quark jet function $J^{(1)r}(m_J^2, k_J^0, R)$, where the R dependence is introduced by requiring the real gluon to be emitted within the jet cone of radius R, and $\hat{n}_{b+g}$ denotes the direction of the total momentum of the b quark and the real gluon. The separation of the fermion flow and the color flow is also achieved by applying Eqs. (7) and (9). Combining the three δ functions in Eq. (16) and the phase spaces for the b quark and the gluon, together the normalization factor $1/(k_J^0)^2$, we construct $J^{(1)r}(m_J^2, k_J^0, R)$.

The difference between the original diagram and the effective diagram with the eikonal approximation gives the NLO real heavy-quark kernel $H^{(1)r}$. For this difference, it is understood that the infrared contribution in the top quark decay specifically associated with the b quark has been subtracted. The top quark decay is then calculated as its final states are composed of a jet, a real gluon, and a lepton pair at this order. Consequently, we insert the identity in Eq. (6), and associate the three δ functions in Eq. (6) with the LO b-quark jet function, forming $J^{(0)}(m_J^2 - 2k_J \cdot l, E_J - l^0, R)$. Therefore, the differential decay width is expressed as the convolution

$$d\Gamma^{(1)r}(t \to b\ell\nu)$$
$$= \frac{\sqrt{2}\pi}{(2\pi)^5}\left(\frac{m_t}{2}\right)^3 d\cos\theta_J dm_J^2 \frac{x_J dx_J}{\sqrt{1 - 4z_J/x_J^2}} dx_\ell d\chi$$
$$\times \Bigg[H^{(0)}(k_t, k_\ell, k_J)J^{(1)r}(m_J^2, E_J, R)$$
$$+ \int \frac{d^3l}{2l^0(2\pi)^3} H^{(1)r}(k_t, k_\ell, k_J, l, R)$$
$$\times J^{(0)}(m_J^2 - 2k_J l, E_J - l^0, R) \Bigg], \qquad (17)$$

where the R dependence of $H^{(1)r}$ arises from the subtraction of $J^{(1)r}$ from the QCD diagram. We should include the NLO diagrams into the complete heavy-quark kernel $H^{(1)}$ with the radiative gluons being exchanged among the top quarks. This category contains the virtual diagrams, such as the self-energy correction to the top quark, and the real diagrams, where gluons are exchanged between the top quarks on both sides of the final-state cut. These diagrams are also characterized by the scale m_t, i.e., dominated by the contribution from l not collimated to k_J.

C. Factorization at all orders

To extend the jet factorization to all orders, we follow the procedures outlined in Ref. [13]: we first employ the collinear replacement for the metric tensor of a gluon propagator [13],

$$g^{\alpha\beta} \rightarrow \frac{\xi_J^\alpha l^\beta}{\xi_J \cdot l}, \qquad (18)$$

where the vertex α (β) is located on the b-quark line (all other lines in the QCD diagrams for the differential decay width). It is easy to see that Eq. (18) picks up the leading collinear contribution. Applying the Ward identity to the contractions of l^β [13], it can be shown that all the contractions are summed into the factorized form containing the NLO jet functions $J^{(1)}$ derived in the above subsections. The factor $\xi_J^\alpha/\xi_J l$ in Eq. (18) corresponds to the Feynman rules for the top quark propagator under the eikonal approximation, namely, for the Wilson lines, which are demanded by the gauge invariance of the jet function as a matrix element of a nonlocal operator. Hence, a gluon collimated to the b quark is factorized from the $O(\alpha_s^{N+1})$ diagrams, leading to $d\Gamma^{(N+1)} \approx d\Gamma^{(N)} \otimes J^{(1)}$. At last, we establish the all-order factorization by induction [13],

$$d\Gamma(t \rightarrow b\ell\nu)$$
$$= \frac{\sqrt{2}\pi}{(2\pi)^5}\left(\frac{m_t}{2}\right)^3 d\cos\theta_J dm_J^2 \frac{x_J dx_J}{\sqrt{1-4z_J/x_J^2}} dx_\ell d\chi$$
$$\times H(k_t, k_\ell, k_J, R) J(m_J^2, E_J, R). \qquad (19)$$

The above steps are basically the same as in Ref. [13], so the detail will not be repeated in this work.

To verify that the jet function in Eq. (19) absorbs the correct logarithms, Eq. (12) for virtual corrections and Eq. (22) for real corrections in the "unresolved" region in Ref. [8] are expanded in the small $z_b = m_b^2/m_t^2$ limit, and the large logarithms $\ln^2(z_b/x_b^2)$, with the energy fraction of the b quark $x_b = 2E_b/m_t$, are identified. The coefficients of these large logarithms are then compared to those of $\ln\bar{N}$, with $\bar{N} \equiv N\exp(\gamma_E)$, in the expansion of the Sudakov exponent up to NLO (see Appendix A of Ref. [20]), where the variable N arises from the Mellin transformation in the jet mass space. It is seen that both the double and single logarithms have the same coefficients in the two references, except an additional single logarithm proportional to $\ln(1/x_{min}) - 9/4$ in Ref. [8]. The dimensionless parameter x_{min} was introduced by slicing the phase space of real corrections into the "resolved" and unresolved regions, and the contribution from the former was obtained from a numerical integration. We believe that the additional logarithm proportional to $\ln(1/x_{min}) - 9/4$ should be canceled, once the resolved contribution is also included in the comparison, since the total result is independent of x_{min}. An equivalent postulation is that

$\ln(1/x_{min}) - 9/4$ can be made to vanish by choosing an appropriate value for the arbitrary x_{min}.

As stated in the Introduction, the NLO corrections to the spin analyzing power, being integrated over all final-state phase space, are not important [8]. With the large logarithms having been organized into the jet function, the remaining NLO corrections to the heavy-quark kernel are expected to be negligible. Therefore, we will adopt the LO heavy-quark kernel for numerical analysis below. The differential decay width is then given by

$$\frac{d\Gamma(t \rightarrow b l \nu)}{dm_J^2 dx_J d\cos\theta_J dx_\ell}$$
$$= 2\pi c^{lep} J(m_J^2, E_J, R) f(x_\ell, x_J; z_J)(1 + |\vec{P}|\cos\theta_\ell), \qquad (20)$$

where the χ dependence has been integrated over, and the constant c^{lep} represents

$$c^{lep} = \frac{1}{4}\frac{1}{(2\pi)^4}G_F^2 m_t^5 \xi^2 |V_{tb}|^2. \qquad (21)$$

III. RESULTS

We reexpress Eq. (20) in terms of the polar angle θ_J of the b-quark jet, and the angle $\theta_{J\ell}$ between the momenta of the charged lepton and of the b-quark jet,

$$\frac{d\Gamma(t \rightarrow b\ell\nu)}{dm_J^2 dx_J d\cos\theta_J dx_\ell} = 2\pi c^{lep} J(m_J^2, E_J, R) f(x_\ell, x_J; z_J)$$
$$\times (1 + |\vec{P}|\cos\theta_{J\ell}\cos\theta_J), \qquad (22)$$

with

$$\cos\theta_{J\ell} = \frac{1}{\beta_J}\left[1 - \frac{2(x_\ell + x_J - 1 - z_J)}{x_J x_\ell}\right], \qquad (23)$$

and $\beta_J = \sqrt{1 - 4z_J/x_J^2}$. Further integrating over the energy fractions x_J and x_ℓ, Eq. (22) gives

$$\frac{1}{\Gamma}\frac{d\Gamma}{d\cos\theta_J dz_J} = \frac{1}{2A}[a(z_J) + b(z_J)|\vec{P}|\cos\theta_J], \qquad (24)$$

where A, $a(z_J)$, and $b(z_J)$ are written as

$$A = \int_0^1 dz_J a(z_J),$$
$$\Gamma = 4\pi c^{lep} A,$$
$$a(z_J) = \int_{x_{J\min}}^{x_{J\max}} dx_J J(z_J, x_J, R) F_a(z_J, x_J), \qquad (25)$$
$$b(z_J) = \int_{x_{J\min}}^{x_{J\max}} dx_J J(z_J, x_J, R) F_b(z_J, x_J),$$

with $x_{J\min} = 2\sqrt{z_J}$, $x_{J\max} = 1 + z_J$, and

$$F_a = \frac{x_J \beta_J}{[1 + z_J - x_J - \xi]^2 + (\xi \eta)^2}$$
$$\times \left[-\frac{1}{3} x_J^2 + \frac{1 + z_J}{2} x_J - \frac{2 z_J}{3} \right],$$

$$F_b = \frac{1}{[1 + z_J - x_J - \xi]^2 + (\xi \eta)^2}$$
$$\times \left[-\frac{1}{3} x_J^3 + \frac{1 + 3 z_J}{6} x_J^2 + \frac{4 z_J}{3} x_J - \frac{2}{3} z_J (1 + 3 z_J) \right].$$

$$(26)$$

The R dependencies of $a(z_J)$ and $b(z_J)$ in Eq. (25) are implicit.

The spin analyzing power for a final state i in a polarized top quark decay can be defined via the average of $\cos \theta_i$,

$$\langle \cos \theta_i \rangle \equiv \frac{1}{\Gamma} \int d \cos \theta_i \cos \theta_i \frac{d \Gamma}{d \cos \theta_i}, \qquad (27)$$

with which the usual expression in Eq. (1) leads to $\kappa_i = 3 \langle \cos \theta_i \rangle$. Following the same reasoning, we can study the spin analyzing power for the b-quark jet with a specified invariant mass,

$$\kappa_J(z_J) \equiv 3 \langle \cos \theta_J \rangle = \frac{3}{\Gamma} \int d \cos \theta_J \cos \theta_J \frac{d \Gamma}{d \cos \theta_J d z_J} = \frac{b(z_J)}{a(z_J)}. \qquad (28)$$

That is, the function $a(z_J)$ is related to the decay width for producing a b-quark jet of mass m_J, and the function $b(z_J)$ is related to angular distribution of the b-quark jet. In this paper, we will evaluate $a(z_J)$, $b(z_J)$, and $\kappa_J(z_J)$, and discuss the effect on the spin analyzing power from the inclusion of the jet function.

It has been observed that the b quark mass is negligible in the analysis of the polarized top quark decay according to Ref. [8], implying the approximation of the b-quark jet function by the light-quark jet function. Moreover, it was noticed that the differential cross sections for jet production scale with the ratio $y \equiv m_J/(R E_J)$ [20]. To simplify the numerical calculation, we are allowed to parametrize the light-quark jet function,

$$J(y) = \begin{cases} 0 & \text{for } y \leq y_0, \\ \frac{J_0}{(R E_J)^2} (y - y_0)^{k_1} \exp(-k_2 y^2) & \text{for } y > y_0, \end{cases} \qquad (29)$$

where $1/(R E_J)^2$ fixes the dimension of the jet function. The normalization constant J_0, determined by $\int d m_J^2 J(m_J^2, E_J, R) = 1$, does not affect the evaluation of the spin analyzing power as indicated by Eq. (28). Fitting Eq. (29) to Figs. 4 and 5 in Ref. [20], which have an involved nonperturbative contribution from the region with large Mellin moments, we obtain $J_0 = 491.4$, $y_0 = 0.05$ and $k_1 = 0.6$, and $k_2 = 75$. It should be stressed that the parametrized jet function must have some deviation from the exact one, and the soft function has been neglected here. Hence, results presented below can be regarded as being derived from a theoretically well motivated phenomenological study.

We adopt the following inputs [22]:

$$m_t = 173.5 \,\text{GeV}, \quad m_W = 80.39 \,\text{GeV}, \quad \Gamma_W = 2.085 \,\text{GeV}, \qquad (30)$$

and vary the jet radius to examine its influence by choosing $R = 0.4$, 0.7, and 1.0. The jet mass dependencies of $a(z_J)$ and $b(z_J)$ with three different values of R are displayed in Figs. 5(a) and 5(b), respectively. The peaks arise from the convolutions of the jet function with the kernels F_a and F_b that contain the Breit-Wigner structure in the W-boson propagator. Increasing the jet radius, the peaks of $a(z_J)$ and $b(z_J)$ shift toward the large mass region, and both distributions become broader, because more infrared radiations are included. The peak positions z_J^{peak} (m_J^{peak}), almost identical for $a(z_J)$ and $b(z_J)$, are found to be 2.1×10^{-4} (2.5 GeV), 6.5×10^{-4} (4.4 GeV), and 1.3×10^{-3} (6.3 GeV) with $R = 0.4$, 0.7, and 1.0, respectively. They are of the same order of magnitude as the mass ratio between the b quark and the top quark, $z_b = 5.8 \times 10^{-4}$ for $m_b = 4.18$ GeV.
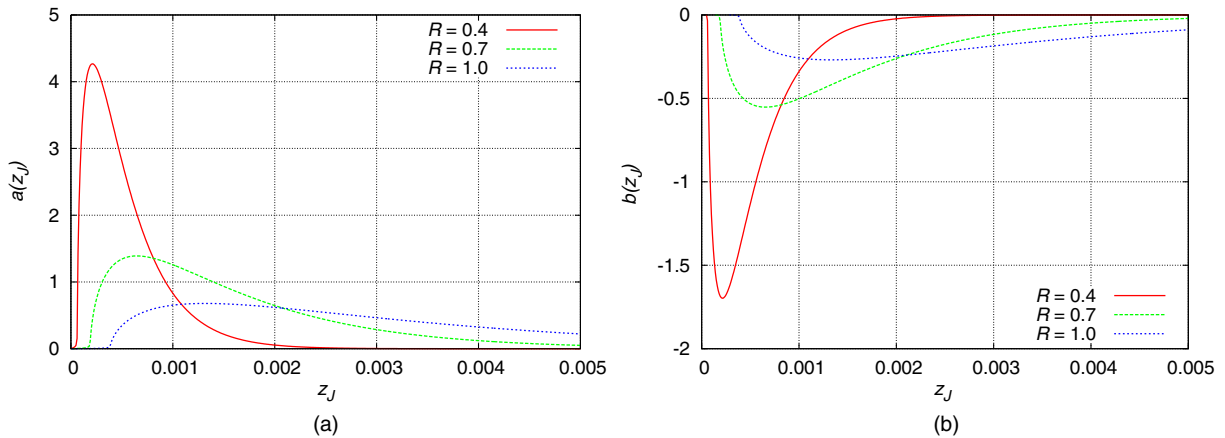

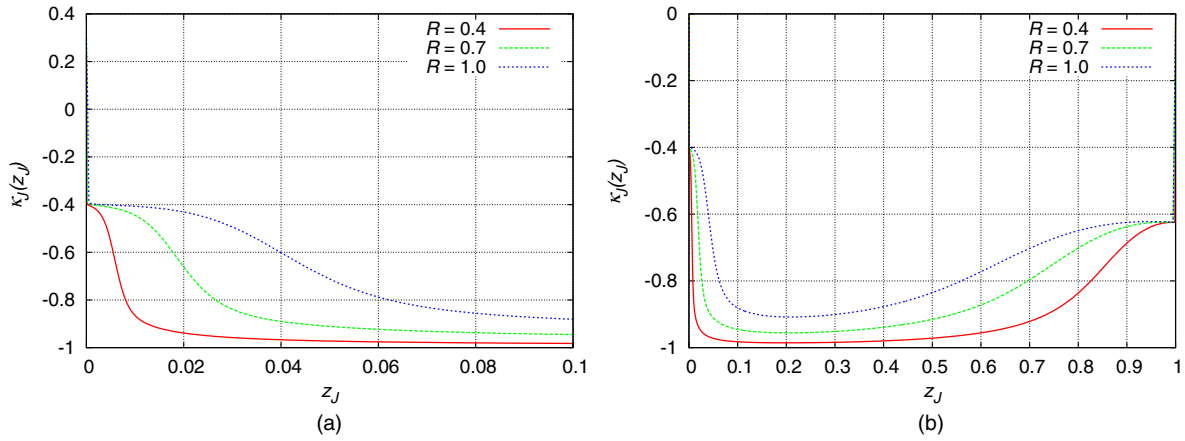FIG. 5 (color online). Dependencies of (a) $a(z_J)$ and of (b) $b(z_J)$ on z_J.

FIG. 6 (color online). Dependence of κ_J on z_J in the ranges of (a) $0 < z_J < 0.1$ and of (b) $0 < z_J < 1$. The ratios $z_J = 0.001, 0.005,$ 0.01, 0.05, 0.1, 0.5, and 1.0 correspond to the jet masses $m_J = 5.5, 12.3, 17.4, 38.8, 54.9, 122.7,$ and 173.5 GeV, respectively.

The dependence of the spin analyzing power $\kappa_J(z_J) = b(z_J)/a(z_J)$ on the jet mass is shown in Fig. 6, with its behavior at small z_J being highlighted in Fig. 6(a). It indicates that all curves agree with $\kappa_J \approx -0.4$ obtained in the literature at $z_J \approx 0$. The spin analyzing power then increases rapidly with the jet mass, stabilizes around $\kappa_J = -0.9 \sim -1$ (depending on the jet radius) in a wide mass region $0.1 < z_J < 0.5$, and slowly decreases at large z_J. At last, the spin analyzing power vanishes quickly at $z_J = 1$ as expected, which corresponds to the kinematic boundary. Another important feature is that $\kappa_J(z_J)$ is insensitive to the choice of the jet radius in the middle mass region. Although the jet production is dominated by the mass region around m_b, it is still possible to determine the spin of a polarized top quark by measuring the angular distribution of the b-quark jet with a bit higher mass. In particular, the broader mass distribution at a larger jet radius warrants this possibility against lower event rates.

We compare κ_J in Eq. (28) based on the jet factorization with the usual spin analyzing power κ_b based on the parton model. Replacing the jet function by its LO expression $\delta(m_J^2 - m_b^2)$, namely, regarding the b quark as a parton, we get the spin analyzing power -0.401. This value is close to the fixed-order (LO or NLO) results in Refs. [6,7] for semileptonic decays and in Ref. [8] for hadronic three-body decays. Integrating $a(z_J)$ and $b(z_J)$ over the jet mass, our formalism reduces to the usual spin analyzing power, giving $-0.407, -0.402,$ and -0.400 for $R = 0.4, 0.7,$ and 1.0, respectively. The above checks confirm the consistency of our formalism.

The possible enhancement of the spin analyzing power by considering the jet function is explained as follows. We first investigate the jet-mass dependence of the ratio F_b/F_a in Fig. 7(a), and observe that $|F_b/F_a|$ for a given x_J decreases with z_J from an initial value at $z_J = 0$. Plotting the x_J dependence of F_a and F_b, it is seen that the curve
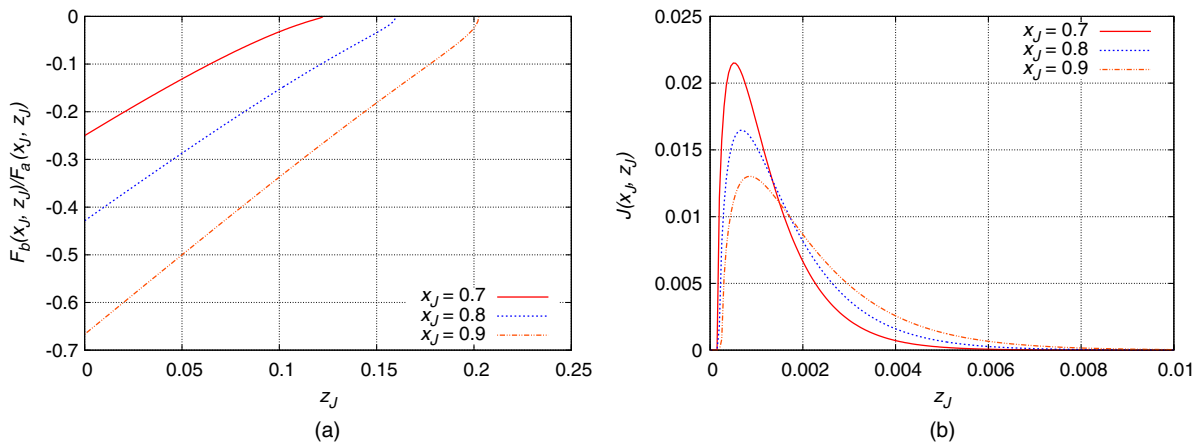

FIG. 7 (color online). Dependencies of (a) the ratio F_b/F_a and of (b) the jet function J with $R = 0.7$ on z_J for $x_J = 0.7, 0.8,$ and 0.9. The peak positions for the jet function are 5.0×10^{-4} (3.9 GeV), 7.0×10^{-4} (4.6 GeV), 8.5×10^{-4} (5.1 GeV), in z_J (m_J) for $x_J = 0.7$, 0.8, and 0.9, respectively.

exhibits a peak at $x_J \approx 0.8$ for a wide range of z_J, namely, $x_J = 0.8$ is a typical jet energy fraction in a top quark decay. It accounts for the usual spin analyzing power derived in the literature, because the initial value is about $F_b/F_a \approx -0.4$ as $x_J = 0.8$. The initial value increases with x_J, and reaches around -0.7 as $x_J = 0.9$. To enhance the spin analyzing power, the large x_J region must be selected. We then display the behavior of the b-quark jet function with $R = 0.7$ in Fig. 7(b), where it exhibits weaker suppression at z_J slightly higher than zero, say, $z_J > 0.002$, as x_J increases. That is, Fig. 7(b) shows the known broadening of a jet in the mass distribution with the jet energy.

Since F_b/F_a with $x_J > 0.8$ gets more weight as convoluted with the jet function, the spin analyzing power grows with z_J. To confirm that the jet energy dependence plays an important role, we test a model jet function, which is energy independent, $J(m_J^2) = \theta(m_0^2 - m_J^2)/m_0^2$. Inserting this simple model into Eq. (25), we obtain the spin analyzing power that always decreases with z_J. It is worthwhile to test experimentally the enhancement of the spin analyzing power through the inclusion of jet dynamics.

IV. CONCLUSION

In this paper we have performed pQCD factorization of the b-quark jet function from the semileptonic decay of a polarized top quark by means of the eikonal approximation and the Ward identity. The resultant formula is expressed as the convolution of the infrared-finite heavy-quark kernel with the jet function, which is dominated by infrared radiations. Adopting the LO heavy-quark kernel and parametrizing the jet function from QCD resummation, we have predicted the dependence of the spin analyzing power associated with the b-quark jet on its invariant mass. It has been verified that our formalism reproduces the fixed-order results by integrating over the jet mass. Our investigation indicated that the spin analyzing power could be possibly enhanced by a factor 2 as measuring the angular distribution of the b-quark jet with a specified invariant mass. The mechanism responsible for the enhancement has been elaborated, which is attributed to the broadening of a jet in the mass distribution with the jet energy. This broadening puts more weight on the contribution from the region with higher jet energy, that intends to give a larger spin analyzing power. The above observation is rather insensitive to the choice of the jet radius, and worthy of experimental confrontation in view of deeper understanding of the effect from including jet dynamics into the polarized top quark decay.

As future works, NLO corrections to the heavy-quark kernel need to be taken into account in order to improve the precision of our predictions. At this level, the dependence of the top quark mass definition on renormalization schemes (for instance, the $\overline{\text{MS}}$ mass [23,24] or the pole mass), becomes an essential issue. It is possible to extend the current formalism to hadronic decays of a polarized top quark, whose analysis is more complicated. Another important direction is to develop the formalism for a boosted top quark at LHC [25,26], that mainly decays into a single jet. Substructures for a polarized top quark jet, which improve the extraction of the information on the top quark polarization, can be calculated.

ACKNOWLEDGMENTS

[1] F.-P. Schilling, Int. J. Mod. Phys. A **27**, 1230016 (2012).
[2] W. Bernreuther, J. Phys. G **35**, 083001 (2008).
[3] J.M. Campbell and R. Keith Ellis, arXiv:1204.1513.
[4] X. Gong, Z.-G. Si, S. Yang, and Y.-j. Zheng, Phys. Rev. D **87**, 035014 (2013); S.M. Troshin and N.E. Tyurin, Mod. Phys. Lett. A **27**, 1250211 (2012); S. Fajfer, J.F. Kamenik, and B. Melic, J. High Energy Phys. 08 (2012) 114.
[5] M. Fischer, S. Groote, J.G. Körner, and M.C. Mauser, Phys. Rev. D **65**, 054036 (2002).
[6] M. Jezabek and J.H. Kühn, Nucl. Phys. **B320**, 20 (1989).
[7] A. Czarnecki, M. Jezabek, and J.H. Kühn, Nucl. Phys. **B351**, 70 (1991).
[8] A. Brandenburg, Z.G. Si, and P. Uwer, Phys. Lett. B **539**, 235 (2002).
[9] M. Jezabek, Nucl. Phys. B, Proc. Suppl. **37**, 197 (1994).
[10] J.C. Collins, D.E. Soper, and G. Sterman, Nucl. Phys. **261**, 104 (1985); **308**, 833 (1988).
[11] G.T. Bodwin, Phys. Rev. D **31**, 2616 (1985); **34**, 3932 (1986).
[12] J.C. Collins and G. Sterman, Nucl. Phys. **185**, 172 (1981).
[13] H.-n. Li, Phys. Rev. D **64**, 014019 (2001); M. Nagashima and H.-n. Li, Eur. Phys. J. C **40**, 395 (2005).
[14] J.C. Collins, Adv. Ser. Dir. High Energy Phys. **5**, 573 (1989).
[15] A.H. Mueller, Phys. Rev. D **20**, 2037 (1979).
[16] J.C. Collins and D.E. Soper, Nucl. Phys. **193**, 381 (1981).
[17] A. Sen, Phys. Rev. D **24**, 3281 (1981).
[18] H. Contopanagos, E. Laenen, and G. Sterman, Nucl. Phys. **484**, 303 (1997).

[19] H.-n. Li, Z. Li, and C.-P. Yuan, Phys. Rev. Lett. **107,** 152001 (2011).

[20] H.-n. Li, Z. Li, and C.-P. Yuan, arXiv:1206.1344.

[21] K. Fujikawa, Prog. Theor. Phys. **61,** 1186 (1979); J. H. Kühn, Acta Phys. Pol. B **12,** 347 (1981); J. H. Kühn and K. H. Streng, Nucl. Phys. **B198,** 71 (1982).

[22] J. Beringer *et al.* (Particle Data Group), Phys. Rev. D **86,** 010001 (2012).

[23] U. Langenfeld, S. Moch, and P. Uwer, Phys. Rev. D **80,** 054009 (2009).

[24] V. Ahrens, A. Ferroglia, M. Neubert, B. D. Pecjak, and L. L. Yang, J. High Energy Phys. 09 (2010) 097.

[25] J. Shelton, Phys. Rev. D **79,** 014032 (2009).

[26] D. Krohn, J. Shelton, and L. T. Wang, J. High Energy Phys. 07 (2010) 041.